A Variational Data Assimilation Algorithm to Estimate Salinity in the Berre Lagoon with Telemac3D

S. Ricci, A. Piacentini, A.T. Weaver
Sciences de l'Univers au CERFACS, URA1875
Toulouse, France
ricci@cerfacs.fr

R. Ata, N. Goutal
Laboratoire national d'Hydraulique et d'Environnement
Chatou, France
riad.ata@edf.fr

Abstract— **Variational assimilation of in-situ data for the description of the salinity field in the Berre lagoon is explored. The Berre lagoon is a receptacle of 1000 Mm^3 where salty water from the Mediterranean Sea meets fresh water discharged by the hydroelectric plant at Saint-Chamas and by natural tributaries. Its dynamics are represented by a 3D hydraulic model that simulates the mean tracer and current fields. This simulation should be further improved to allow for the optimization of the operation of the hydroelectric production while preserving the lagoon ecosystem. A 3D-Var FGAT data assimilation algorithm is used to correct the initial salinity state over a 1-hour time window assimilating observations at three fixed buoys each equipped with 5 XBT sensors in the vertical every 15 minutes. The minimization is performed in a space spanned by vectors of the size of the observation vector in order to reduce both memory usage and computational cost. The background error covariance matrix for salinity is modelled using a diffusion operator. The sequential correction of the salinity state improves the representation of the strongly stratified salinity field over the assimilation window as well as in the short-term forecast. The sensitivity of the assimilation to the background error horizontal and vertical length scale was investigated in single observation experiments as well as in a real case study.**

I. INTRODUTION

The Berre lagoon is a receptacle of 1000 Mm^3 where salty water from the Mediterranean Sea, through the Canal de Caronte, meets fresh water discharged by the hydroelectric plant at Saint-Chamas and by natural tributaries (Arc and Touloubre rivers). The Laboratoire National d'Hydraulique et d'Environnement (LNHE) aims at optimizing the operation of the hydroelectric production while preserving the lagoon ecosystem. To achieve this objective, improving the quality of the simulation and more specifically the description of the salinity state is essential. The hydrodynamics of the lagoon is modelled with a 3D resolution of the shallow water equations using the TELEMAC-3D (T3D) software developed by Electricité De France (EDF R&D) coupled with the water quality model DELWAQ developed by DELTARES. The proper representation of the stratified salinity and temperature fields as well as the 3D currents was identified as a valuable research objective with direct applications for both electricity production and ecological matters. These fields drive the time of residency for the water masses in the lagoon and thus the phytoplantonic bloom. Indeed, the haline stratification is intensified by the inflow of the salty waters from the Mediterranean Sea and of the fresh waters from the hydroelectric power plant. The deep waters are thus anoxied and the nutriments are trapped in the deep waters of the lagoon. When the wind blows, mixing occurs, the entire water column is oxigenized and the nutriments are consumed by the phytoplancton. Three fixed buoys in the lagoon and one in the Canal de Caronte are equipped with five XBT (eXpendable BathyThermograph) sensors along the vertical that measure the temperature and salinity every 15 minutes. These data are gathered by the GIPREB (Groupement d'Intérêt Public pour la Réhabilitation de l'étang de Berre) and allow, since 2005, the European Comission to ensure that France is applying the decree issued in 1987 to protect the Mediterranean waters against pollution.

Preliminary studies on the calibrated 11 vertical plan T3D model [1] were carried out to quantify the difference between a reference simulation and the observations on a test period. Most uncertainty comes from the maritime, fluvial and meteorological boundary conditions. More specifically the fresh water input from the Touloubre and the Arc influents is under-estimated, some fresh water inputs from minor influents are neglected and the evapotranspiration is over-estimated. The temporal variability of these errors in fresh water inputs was partly corrected by adding an artificial input at Caronte ranging from 3.5 to 15 m^{3}s^{-1}. With this correction, the lagoon mean salinity drift was reduced by 30% over September-December 2006. Still, the temporal intra- and inter-annual variability of this artificial correction is difficult to estimate and the hydraulics state simulated by the model remains imperfect: the currents tend to be under-estimated and the difference between the simulated salinity and the observations can reach up to several g/l. These uncertainties could be corrected with a data assimilation (DA) algorithm.

Significant advances have been made in recent years in hydraulic DA for water level and discharge prediction [2], as well as for parameter estimation [3], using in-situ as well as remote sensing data [4]. Recent studies have showed the benefits that hydrology and hydraulics can draw from the progress of DA approaches using either variational methods [5], particle filtering [6], Extended Kalman Filter [7], Ensemble Kalman filter for state updating [8], or for dual state-parameter estimation [9]. Some studies are formulated in an operational setting and demonstrate the performance gained from DA for operational flood and inondation forecasting [10,11,12]. DA offers a convenient framework for integrating observations into a numerical model in order to provide optimal estimates of poorly known parameters and simulated model states and thus, to improve predictions. The key idea is that, when used alone, neither measurements nor numerical models can provide a reliable and complete description of the real state of the physical system. While the merits of DA have been largely demonstrated in the global and coastal ocean fields [13,14] they are yet to be fully taken advantage of in lakes and lagoon hydrodynamical modelling systems.

In this paper, a collaborative work between LNHE and CERFACS (Centre Européen de Recherche et de Formation Avancée en Calcul Scientifique) is described to develop a DA algorithm for T3D that exploits the continuous in-situ salinity measurements at three locations in the Berre lagoon. Similarly to the meteorological and oceanographic approaches [15], the observations are used sequentially to update the hydrodynamic state. More specifically, a 3D-Var FGAT algorithm presented in Section 2, is used to correct the salinity state at the beginning of an assimilation window (or cycle) over which several observations are available. This incremental variational assimilation algorithm relies on the hypothesis that corrections to the model state are approximately constant over a chosen time window. Sensitivity experiments show that in order to cope with this constraint, the analysis time window should be at most 3h. With the current T3D Berre model, as the number of observations over an assimilation window is significantly smaller than the size of the model state vector (less than 100 observations compared to approximately 70000 cells), the minimization is performed in a space spanned by vectors of the size of the observation vector. This allows us to reduce significantly both memory usage and computational cost [16]. The background error covariance matrix for salinity is modelled using a diffusion operator [17]. Preliminary results from the 3D-Var FGAT system are presented in Section 3. The sequential correction of the salinity state improves the representation of the strongly stratified salinity field over the assimilation window as well as in the short-term forecast. The sensitivity to the horizontal and vertical length scale was investigated in single observation experiments as well as in a real case study.

II. Variational Data Assimilation Algorithm

3D-Var FGAT (3D variational method with First Guess at Appropriate Time) can be derived as a simplification of 4D-Var in which the temporal dependence of the analysis is neglected. The 4D-Var algorithm formulates the difference between the numerical model outputs and the observations over the assimilation window $[t_0,t_T]$ as a function of the initial state of the system $\mathbf{x}=\mathbf{x}(t_0)$, called the control vector (n-dimensional). This cost function is regularized by a background term that penalizes the distance to the background state $\mathbf{x}^b$ which is the model estimate of this initial condition (prior to the assimilation). The statistics of its errors are described by the background error covariance matrix $\mathbf{B}$. The observation vector $\mathbf{y}^o$ is a vector of size N that gathers the observations available in space and time over the assimilation window. The statistics of its errors are described by the observations error covariance matrix $\mathbf{R}$ (assumed to be diagonal in the following). The inverse of the background and observation covariance error matrices define the weighting matrices of the quadratic terms in the cost function

$$\mathrm{J}(\mathbf{x}) = \frac{1}{2}(\mathbf{x}-\mathbf{x}^b)^T\mathbf{B}^{-1}(\mathbf{x}-\mathbf{x}^b)+\frac{1}{2}(G(\mathbf{x})-\mathbf{y}^o)^T\mathbf{R}^{-1}(G(\mathbf{x})-\mathbf{y}^o). \quad (1)$$

In order to compute the model equivalent of the observation vector, the initial state $\mathbf{x}$ is propagated over the assimilation window by the dynamical model $M_{t0,tT}$, then mapped to the observation space using the observation operator H. The composition of H and $M_{t0,tT}$ is the generalized observation operator denoted by G; it is non linear as the dynamical model is non linear with respect to the control vector. The initial state that minimizes the cost function is called the analysis $\mathbf{x}^a$. It can be integrated forward in time to produce a forecast beyond the assimilation time window.

The minimization of the non-quadratic cost function J is usually achieved as a sequence of minimizations of approximated quadratic functions where a local linearization of the generalized observation operator is used. This is the incremental formulation that aims at identifying a correction $\delta\mathbf{x}$ to the background state such that $\mathbf{x}^a = \mathbf{x}^b + \delta\mathbf{x}^a$. The generalized observation operator is linearized around a reference state, usually chosen as the background, that requires the formulation of the tangent-linear $\mathbf{M}_{t0,tT}$ and $\mathbf{H}$ of the nonlinear model $M_{t0,tT}$ and of the observation operator H with respect to $\mathbf{x}$ so that

$$\mathbf{G}(\mathbf{x}) = \mathbf{H}\,\mathbf{M}_{t0,tT}. \quad (2)$$

The incremental cost function J_{inc} reads:

$$\mathrm{J}_{inc}(\delta\mathbf{x}) = \frac{1}{2}\delta\mathbf{x}^T\mathbf{B}^{-1}\delta\mathbf{x}+\frac{1}{2}(\mathbf{G}\delta\mathbf{x}-\mathbf{d})^T\mathbf{R}^{-1}(\mathbf{G}\delta\mathbf{x}-\mathbf{d}) \quad (3)$$

where $\mathbf{d}$ is the innovation vector that denotes the difference between the observation vector and the background trajectory integrated from the background state with $M_{t0,tT}$. The 3D-Var FGAT algorithm lies on the hypothesis that the tangent-linear $\mathbf{M}_{t0,tT}$ can be approximated by the identity matrix, meaning that the dynamics of a perturbation to the state vector is represented by a persistence model. The first reason for choosing this approach is that, as of today, the tangent-linear model of T3D with respect to the initial state is not yet available. The second reason is that the cost of the 3D-Var FGAT is much smaller than that of the 4D-Var while still

providing satisfying results (for instance in the fields of meteo and ocean) when the **B** is properly described.
The exact solution of (3) is obtained by setting the gradient of J_{inc} to zero, which yields [18]

$$\delta\mathbf{x}^{a} = (\mathbf{B}^{-1} + \mathbf{G}^{T}\mathbf{R}^{-1}\mathbf{G})^{-1}\mathbf{G}^{T}\mathbf{R}^{-1}\mathbf{d}. \quad (4)$$

Since the matrices in (4) are large and only available in operator form (i.e., as a matrix-vector product), an approximate solution is usually found by iteratively solving a linear system. The minimization of J_{inc} can either be solved in the primal space spanned by vectors of the size of the model control vector, or, using the Sherman-Morrison-Woodbury formula [19], in the dual space spanned by vectors of the size of the observation vector. The dual approach is advantageous in the present study since the size of observation space is significantly smaller than the size of the control vector. The analysis in the dual formulation reads

$$\delta\mathbf{x}^{a} = \mathbf{B}\,\mathbf{G}^{T}(\mathbf{G}\mathbf{B}\,\mathbf{G}^{T} + \mathbf{R})^{-1}\mathbf{d} \quad (5)$$

which is solved iteratively with a conjugate gradient method applied to the N*N linear system

$$(\mathbf{G}\mathbf{B}\,\mathbf{G}^{T} + \mathbf{R})\lambda = \mathbf{d} \quad \text{and} \quad \delta\mathbf{x} = \mathbf{B}\,\mathbf{G}^{T}\lambda. \quad (7)$$

This linear system can be preconditioned by $\mathbf{R}^{-1}$ in order to accelerate the convergence. The algorithm is known as PSAS [20]. A prohibitively large number of iterations may be required to obtain an acceptable solution with PSAS. [21] proposed an alternative way to solve this problem while ensuring that during the minimization process the current iterate is the same as the one found when minimizing in the primal space with a conjugate gradient algorithm preconditioned by **B**. The details and the implementation of this algorithm called RBCG are given in [16].

The **B** operator is described by the integral equation

$$B(\varsigma(\mathbf{z})) = \int B(\mathbf{z},\mathbf{z}')\,\varsigma(\mathbf{z}')\,d\mathbf{z}' \quad (8)$$

with $\mathbf{z}=(z_1, z_2, z_3)$ representing the spatial directions and $B(\mathbf{z},\mathbf{z}')$ the covariance function for any variable $\zeta(\mathbf{z})$. The modelling of the covariances is usually separated into two operators: one for the variance and one for the correlations. The correlation operator is modelled using an implicitly formulated 3D diffusion equation. This method and its implementation with an implicit scheme are presented in [22]. In the present framework, the correlation functions are described applying the diffusion operator with different diffusion coefficents in the vertical and horizontal directions that relate to the vertical and horizontal correlation length scales. Ad-hoc estimates (isotropic and homogeneous) for these length-scales are used here but objective estimates should be further investigated with an ensemble approach.

III. RESULTS

A. *Single observation validation experiment*

In order to validate the 3D-Var FGAT algorithm, a single observation is assimilated at the closest grid point to SA1 (point A), at -5m deep for January 1st 2008 with a diagonal **B** matrix. Here, the DA procedure comes down to computing a weighted average where the background and observation weights are given by the background and observation error variances. When these are both arbitrarily set to 0.25 psu^2, and given that the observed salinity is equal to 26.434100 psu while the simulated salinity is 26.6386 psu, the analysis increment given by the RBCG (Restricted B-preconditioned Conjugate Gradient) minimization is $\delta\mathbf{x}$ =-0.1022501 psu, which is, as expected half of the BmO (Background Minus Observation computed for salinity) value. It should be noted that the RBCG converges in one single iteration and it was also verified that when the variances are modified, the analysis changes accordingly: it remains close to the background when the observation error variance increases and gets closer to the observation when the background error variance increases.

When the **B** matrix is not diagonal, the difference between the simulated and observed salinity at the observation points translates into a correction at the neighbouring points. The horizontal and vertical spatial repartition of the information is prescribed by the background error correlation functions; more specifically by the horizontal and vertical correlation length-scales L_h and L_v. Fig. 1 presents the horizontal correlation function for point A when L_h=600m. It should be noted that the 0.5 isocontour plotted in white describes a circle of radius equal approximately to 600m, centered in A. It should also be noted that the maximum correlation in A is not exactly equal to 1 (as it should be in theory) because of a normalization procedure within the diffusion operator method that is beyond the scope of this paper.

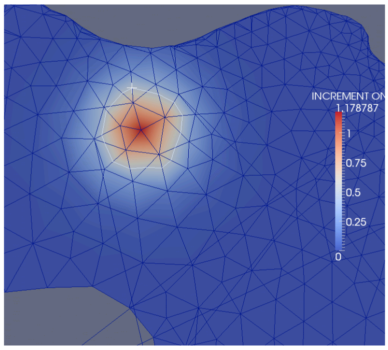

Figure 1: Correlation function (dimensionless) prescribed for point A with L_h=600m over the Berre Lagoon area where SA1 is located.

Similarly, the vertical repartition of the increment relates to L_v that prescribes the shape of the vertical correlation function. The increment is presented in Fig. 2 when L_v=0.5m.

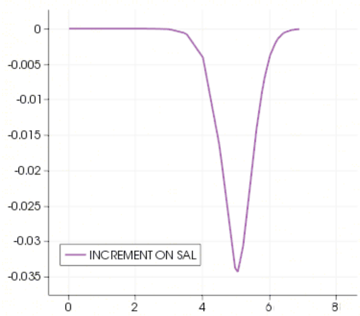

Figure 2: Salinity increment (in psu, on the y-axis) for the single observation experiment, plotted at point A along the vertical (in m, on the x-axis).

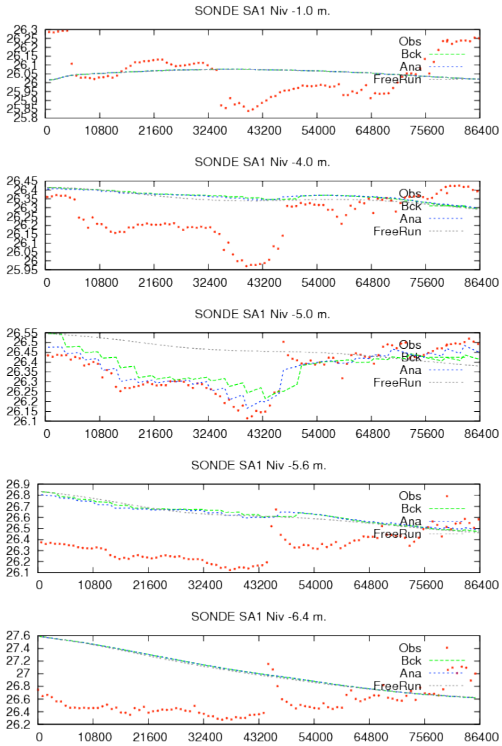

a-

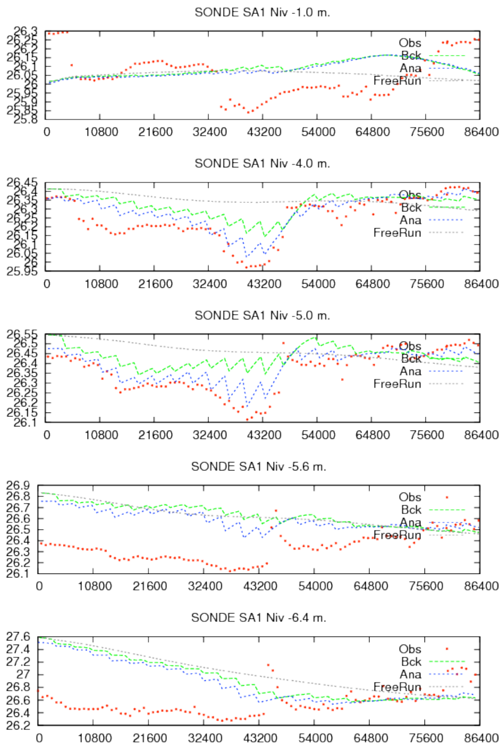

b-

Figure 3: Salinity (in psu) at the 5 observation points at SA1 along the vertical for L_h=200m, a- L_v=0.5m and b- L_v=2m over 24 assimilation cycles of 1 hour. Only the observation at 5m deep are assimilated.

In the following, the observations are used at their real measurement location (generally, not at a grid point), meaning that the computation of BmO implies a spatial interpolation (horizontal and vertical) that represents the observation operator *H* presented in Section 2.

The observations at SA1, at 5 m deep are now assimilated every 15 minutes with an assimilation window of 1 hour, meaning that a correction to the initial salinity state is computed from the 3D-Var FGAT algorithm using 4 observations in the minimization process. This analysis is cycled over 24 hours and the results are presented in Fig. 3a- for L_h=200 m and L_v=0.5 m and in Fig. 3b- for L_h=200 m and L_v=2 m. For each panel, the salinity is represented at SA1, at different vertical depths that correspond to the 5 XBT sensors positions, as a function of time over 24 h, at observation times only. The observations are represented in red, the T3D Free Run (no assimilation) is plotted in black, the background (for the current cycle) is plotted is green and the analysis is plotted in blue. First, it should be noted that at 5 m deep (where the observations are assimilated), the salinity is significantly improved and brought closer to the observations (the background and observation errors variances are set to 4 psu^2). The difference between the analysis and the observation is systematically reduced at the beginning of the assimilation window when the correction is applied, then the model is integrated over 1 hour and deviates from the observations. The analysis salinity value at the end of the assimilation window is the background initial salinity state for the following cycle. The 1-hour integration of the background state can thus be considered as a 1-hour prevision following the 1-hour assimilation window. It should then be noted that the 3D-Var FGAT algorithm improves the salinity over the assimilation period as well as over a forecast period of 1 hour.

When L_v=0.5 m (Fig. 3a-), the assimilation of the observations at 5m deep has no impact on the rest of the water column at SA1 where no observations are assimilated. On the contrary, when L_v=2 m (Fig. 3b-), the salinity is corrected over the entire water column. Whether this correction improves or not the salinity depends on the coherence between the spatial correlation of the errors in the simulated salinity field and the correlation function prescribed in **B**. It also depends on the dynamics of the increment injected at the initial time, this issue will be addressed in the next subsection. Finally, it should be noted that the minimization for each cycle now converges in a small number of iterations, the cost function J_{inc} (3) is reduced and its gradient is brought to zero.

B. *Real-case study: Assimilation of all SA1 observations*

Fig. 4a- displays the results of the assimilation of all the observations at SA1 for the 5 vertical levels, over 24 hours with a 1-hour assimilation window when L_h=200m and L_v=0.5 m. At each level, the salinity is brought closer to the observations over the assimilation and the forecast period. Still, it should be noted that the effect of the increment applied at the beginning of the cycle can lead to an over-correction as observed at 1m deep for t in [54000 s, 72000 s] where the forecast (the background plotted in green) exceeds the Free Run so that the distance to the observation is increased by the DA procedure. This might be due to the too simple description of L_v that is here constant along the vertical and too large close to the surface as the salinity errors in the mixed layer (down to 3 or 4 m deep) are weakly correlated with the salinity errors in sub-surface where the stratification is strong. Under the mixed layer, as the salinity errors are strongly correlated, the correction from the assimilation at one level has a positive impact on the other levels. In order to account for the spatial variability of the salinity errors in the DA process, on-going developments aim at allowing for an inhomogeneous description of the correlation length scales. Preliminary tests showed that the spurious correction at 1m is significantly reduced when L_v=0.25 m, but on the other hand, the improvement for deeper level is slighlty reduced as illustrated in Fig. 4b-.

The 3D-Var FGAT salinity increment for the first assimilation cycle at 1 m deep is shown in Fig. 5a- for L_h=600 m and L_v=0.25 m and the resulting corrected salinity field at the t=0 s is shown in b-. The pink triangle represents the T3D grid element that contains the observation point SA1. As expected, the spatial repartition of the correction is prescribed by the correlation length scale, still the evolution of this increment when the model is integrated from the corrected initial condition should be further investigated as spurious changes to other variables as the pressure, temperature and current could occur thus leading to over corrections. A common way to limit these effects is to spread the correction over the assimilation window instead of applying it, at once, at the initial time for the cycle. This procedure, called IAU Incremental Analysis Updates), was implemented with a basic division of the correction in equal increments applied at each time step over the 1-hour assimilation window. It allows to significantly reduce the over-correction at 1m deep (not shown here) and the shape of the repartition function should be further investigated.

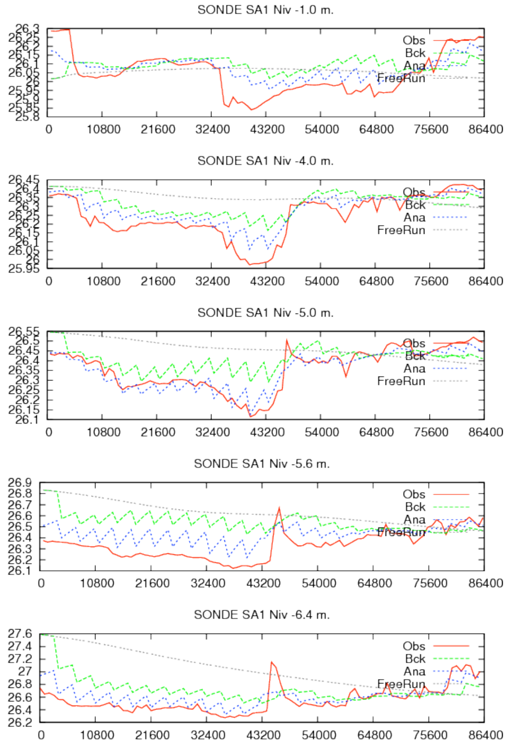

a-

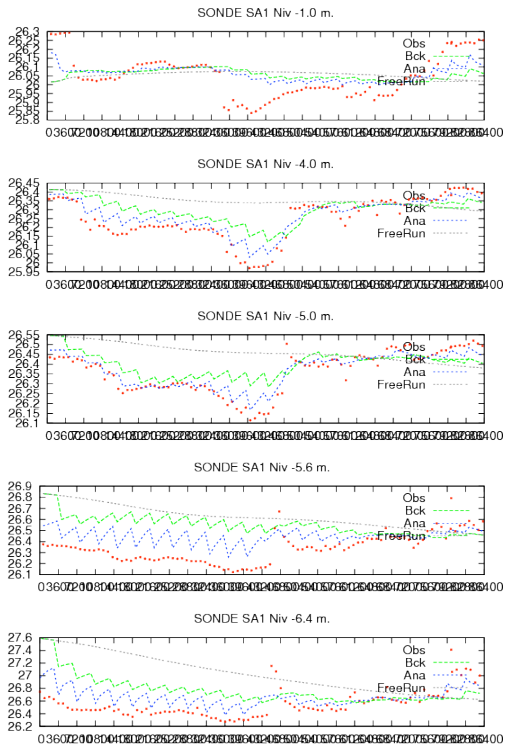

b-

Figure 4: Salinity (in psu) at the 5 observation points at SA1 along the vertical for L_h=200m, a- L_v=0.5m and b- L_v=0.25m over 24 assimilation cycles of 1 hour. All observations at SA1 are assimilated.

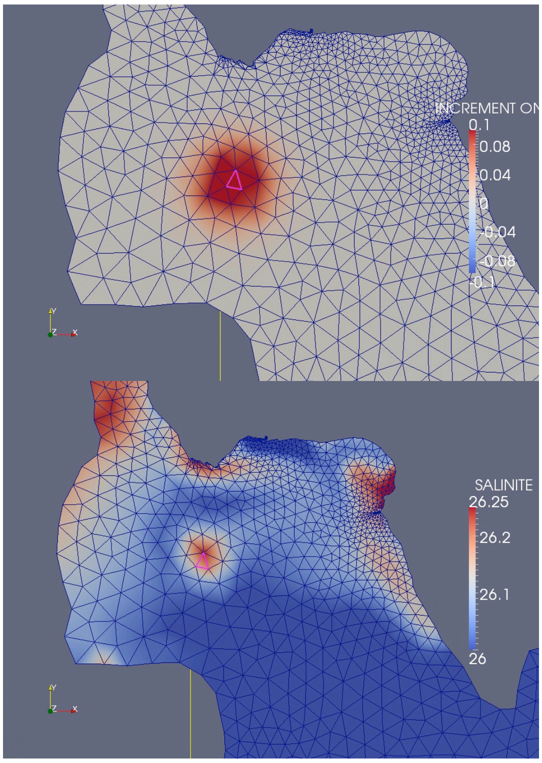

Figure 5: Salinity increment (in psu) for the first assimilation cycle a- L_h=600m and L_v=0.25m, b- analysis salinity field (in psu) for L_h=600m and L_v=0.25m.

CONCLUSION

A 3D-Var FGAT algorithm was implemented in the dual space in order to improve the salinity field description assimilating in-situ salinity observations with a T3D model for the Berre lagoon. The analysis is achieved over a 1-hour window and is applied sequentially every hour. It was shown that the corrected field is closer to the observations over the assimilation and 1-hour forecast periods at the assimilation points. The horizontal and vertical spread of the correction around the observation point depends on the correlation length-scales prescribed in the background error covariance matrix modelled using an implicit 3D diffusion operator. The impact of the vertical length scale was studied and it was shown that in order to avoid spurious correction between the vertical assimilation locations, the correlation length scale should be depth-dependent. This could be achieved using a ensemble-based estimate of the correlation length-scales, eventually with a temporal variability. In further work, the evolution of the salinity increment over time should also be investigated in order to verify that the balance between the other state variables (temperature, currents) is preserved.

REFERENCES

[1] N. Durand, E. Razafindrakoto. "Synthèses et conclusions des études sur la modélisation numérique TELEMAC-3D de l'évolution des courants, de la salinité et de la température dans l'étang de Berre." , Note Interne EDF-LNHE, H-P74-2011-02289-FR, 2011.

[2] Schumann, G., Bates, P.D., Horritt, M.S., Matgen, P., and Pappenberger, F.: Progress in integration of remote sensing-derived flood extent and stage data and hydraulic models, Rev. Geophys., 47, RG4001, doi:10.1029/2008RG000274, 2009.

[3] Durand, M., Lee-Lang, F., Lettenmaier, D.P., Alsdorf, D.E., Rodriguez, E., and Esteban-Fernandez, D.: The Surface Water and Ocean Topography Mission: Observing Terrestrial Surface Water and Oceanic Submesoscale Eddies, IEEE, 98, 766--779, 2010.

[4] Neal, J., Schumann, G., Bates, P., Buytaert, W., Matgen, P., and Pappenberger, F.: A data assimilation approach to discharge estimation from space, Hydrol. Process., 23, 3641-–3649. doi: 10.1002/hyp.7518, 2009.

[5] Valstar, J.R., McLaughlin, D.B., te Stroet, C.B.M., and van Geer, F.C.: A representer-based inverse method for groundwater flow and transport applications, Water Resour. Res., 40, W05116, doi:10.1029/2003WR002922, 2004.

[6] Matgen, P., Montanari, M., Hostache, R., Pfister, L., Hoffmann, L., Guingla, D.P., Pauwels, V., De Lannoy, G., De Keyser, R., and Savenije, H.H.G.: Towards the sequential assimilation of SAR-derived water stages into hydraulic models using the Particle Filter: proof of concept, Hydrol. Earth Syst. Sci, 14, 1773--1785, 2010.

[7] Thirel, G., Martin, E., Mahfouf, J.-F., Massart, S., Ricci, S., and Habets, F.: A past discharges assimilation system for ensemble streamflow forecasts over France, Hydrol. Earth Syst. Sci., 14, 1623--1637, 2010.

[8] Weerts, A.H., and El Serafy, G.Y.H.: Particle filtering and ensemble Kalman filtering for state updating with hydrological conceptual rainfall-runoff models, Water Resour. Res., 42, W09403, doi:10.1029/2005WR004093., 2006.

[9] Moradkhani, H., Sorooshian, S, Gupta, H.V., and Houser, P.-R.: Dual state-parameter estimation of hydrological models using ensemble Kalman filter, Advances in Water Resources, 28, 135--147, 2005a.

[10] Madsen, H., and Skotner, C.: Adaptive state updating in real-time river flow forecasting - a combined filtering and error forercasting procedure, J. Hydrol., 308, 302--312, 2005.

[11] Jean-Baptiste, N., Malaterre, P.-O., Dorée, C. and Sau, J.: Data assimilation for real-time estimation of hydraulic states and unmeasured perturbations in a 1D hydrodynamic model, Journal of Mathematics and Computers in Simulation, Vol. 81, Issue 10, 2201-2214, 2011.

[12] Ricci, S., Piacentini, A., Thual, O., Le Pape, E., and Jonville, G.: Correction of upstream flow and hydraulics state with data assimilation in the context of flood forecasting, Hydrol. Earth Syst. Sci, Vol. 15, 1--21, 2011.

[13] Weaver A.T., Vialard J., Anderson D.L.T.: Three- and four- dimensional variational assimilation with a general circulation model of the tropical Pacific ocean. Part 1: formulation, internal diagnostics and consistency checks. Mon. Weather Rev. 131: 1360-–1378, 2003.

[14] Moore, A.M., Arango H.G., Broquet G., Powell B.S., Zavala-Garay J., Weaver A.T.: The Regional Ocean modelling System (ROMS) 4-dimensional variational data assimilation systems. Part I: System overview and formulation. Prog. Oceanogr. 91: 34–49, 2011a.

[15] Daley, R.: Atmospheric data analysis. Cambridge atmospheric and space science series. Cambridge University Press, 1991.

[16] Gurol, S., A. T. Weaver, A. M. Moore, A. Piacentini, H. G. Arango and S. Gratton. " B-Preconditioned Minimization Algorithms for Variational Data Assimilation with the Dual Formulation", Q. J. R. Meteorol. Soc. , in print.

[17] Weaver, A.T, P. Courtier, P.: Correlation modelling on the sphere using a generalized diffusion equation, Q. J. R. Meteorol. Soc., 127, 1815--1846, 2001.

[18] Tarantola A.: Inverse Problem Theory and Methods for Model Parameter Estimation. SIAM, Philadelphia, 2005.

[19] Nocedal, J., Wright, S.J.: Numerical Optimization. Series in Operations Research, Springer Verlag: Heidelberg, Berlin, New York, 2006

[20] Cohn, S., Da Silva, A., Guo, J., Sienkiewicz, M., Lamich, D.:Assessing the effects of data selection with the DAO physical-space statistical analysis system. Mon. Weather, 126, 2913--2926, 1998.

[21] Gratton, S., Tshimanga, J.: An observation-space formulation of variational assimilation using a Restricted Preconditioned Conjugate-Gradient algorithm. Q. J. R. Meteorol. Soc., 135, 1573-–1585, 2009.

[22] Mirouze, I., Weaver, A.T.: Representation of correlation functions in variational assimilation using an implicit diffusion operator. Q. J. R. Meteorol. Soc., 136, 421--1443, 2010.